# Exact Distributed Stochastic Block Partitioning

Frank Wanye
*Dept. of Computer Science*
*Virginia Tech*
Blacksburg, VA, USA
wanyef@vt.edu

Vitaliy Gleyzer
*MIT Lincoln Laboratory*
Lexington, MA, USA
vgleyzer@ll.mit.edu

Edward Kao
*MIT Lincoln Laboratory*
Lexington, MA, USA
edward.kao@ll.mit.edu

Wu-chun Feng
*Dept. of Computer Science*
*Virginia Tech*
Blacksburg, VA, USA
wfeng@vt.edu

*Abstract*—Stochastic block partitioning (SBP) is a community detection algorithm that is highly accurate even on graphs with a complex community structure, but its inherently serial nature hinders its widespread adoption by the wider scientific community. To make it practical to analyze large real-world graphs with SBP, there is a growing need to parallelize and distribute the algorithm. The current state-of-the-art distributed SBP algorithm is a divide-and-conquer approach that limits communication between compute nodes until the end of inference. This leads to the breaking of computational dependencies, which causes convergence issues as the number of compute nodes increases and when the graph is sufficiently sparse. To address this shortcoming, we introduce EDiSt — an exact distributed stochastic block partitioning algorithm. Under EDiSt, compute nodes periodically share community assignments during inference. Due to this additional communication, EDiSt improves upon the divide-and-conquer algorithm by allowing it to scale out to a larger number of compute nodes without suffering from convergence issues, even on sparse graphs. We show that EDiSt provides speedups of up to 26.9× over the divide-and-conquer approach and speedups up to 44.0× over shared memory parallel SBP when scaled out to 64 compute nodes.

*Index Terms*—community detection, graph clustering, stochastic blockmodels, bayesian inference, asynchronous Gibbs, MPI

## I. INTRODUCTION

Much of the data that is collected today contains entities that are connected to each other. For example, in Internet traffic data, network nodes communicate with each other via packets, while in social media data, people interact with each other's posts and add each other to contact lists. Such data can be represented in the form of a graph, where the entities are represented by a graph's vertices, and the relationships between the entities are represented by the edges between

vertices. Often, these vertices form structural groups called communities, such that the vertices within each group are more closely connected to each other than they are to vertices in other groups. The process of identifying these groups is referred to as community detection [1].

Due to the expressive nature of the graph representation, and the ubiquity of community structure in real-world graph data, community detection has a lot of applications across a wide variety of fields. These fields include bioinformatics, where community detection has been used to aid in identifying carcinogenic gene combinations [2], communication networks, where community detection can be used to aid in the placement of servers [3], and artificial intelligence, where community detection can be used as a pre-processing step that leads to improved classification accuracy [4], [5]. The proliferation of these use cases has led to a lot of interest in research involving community detection.

Optimal community detection is an NP-hard problem. Hence, various heuristics are used to approximate the community structure of a graph [1]. One such heuristic is stochastic blockmodel inference [6]. This heuristic involves building a blockmodel, a latent model of the inter-community connectivity in a graph [7], and then iteratively perturbing this model to find the combination of the number of communities and vertex-to-community assignments that minimize the description length of the blockmodel.

Stochastic block partitioning (SBP) [6], [8] is a community detection algorithm based on stochastic blockmodel inference. It is of interest to the research community because, unlike community detection methods that are not based on inference, SBP does not struggle to identify statistically significant communities [9]. For example, modularity-based methods often exhibit a form of overfitting, leading to the identification of spurious communities in random graphs without planted communities [10]. Inference-based methods, on the other hand, would conclude that such random graphs have no community structure.

SBP is also highly accurate even when the graph community structure is complicated by highly varied community sizes, varied degree distributions within communities, and a high degree of inter-community connectivity, as can be seen by comparing the results obtained in the IEEE/Amazon/MIT Graph Challenge [11]. However, SBP is slower than competing community detection algorithms based on other heuristics and

difficult to parallelize owing to the fact that it is based on an inherently sequential Markov chain Monte Carlo algorithm [11].

There have been several attempts to accelerate SBP through sampling [12], shared memory parallelism [13], and various optimizations [14]. However, for the runtime of SBP to be practical on large-scale, real-world graphs, which often consist of upwards of millions of vertices and edges, the computation needs to be distributed across multiple compute nodes.

To the best of our knowledge, only one distributed implementation of stochastic block partitioning exists: the divide-and-conquer approach described in [15], henceforth abbreviated as DC-SBP. DC-SBP works similarly to the Map-Reduce paradigm, with no communication between compute nodes until the "Reduce" phase, where partial results are combined. Our testing of DC-SBP reveals that is suffers from convergence issues that lead to severe degradation in the quality of community structure that it infers *and* limit the number of compute nodes that DC-SBP can scale to while maintaining accuracy (see Section V-B).

Here we introduce a novel <u>e</u>xact <u>di</u>stributed <u>st</u>ochastic block partitioning (EDiSt[1]) algorithm that does *not* suffer from these convergence issues owing to the introduction of periodic inter-node MPI communication during the course of inference. Thus, EDiSt enables distributed SBP on larger computational clusters and on a larger variety of graphs without sacrificing result quality. Note that the usage of "exact" in EDiSt refers to the algorithm's ability to maintain accuracy at scale and is not a reference to exact community detection, which remains an NP-hard problem. The differences between DC-SBP and EDiSt are summarized in Table I.

TABLE I
DIFFERENCES BETWEEN EDIST AND DC-SBP

| Parameter | DC-SBP | EDiSt |
|---|---|---|
| Data handling | Round-robin data distribution | Data duplication |
| Inter-node communication | Limited to partial result re-combination | Periodic throughout inference |
| Retains accuracy beyond 16 MPI ranks | No | Yes |
| Retains accuracy on sparse graphs | No | Yes |

We summarize our main contributions as follows:

- An empirical analysis demonstrating convergence issues in the state-of-the-art divide-and-conquer distributed stochastic block partitioning as the number of MPI tasks increases and when the graph is sufficiently sparse.
- A novel distributed stochastic partitioning algorithm — EDiSt. We empirically show that EDiSt does not suffer from convergence issues under the same conditions as the divide-and-conquer approach, which allows it to make use of more computational nodes and run on a larger variety of graphs without sacrificing result quality.

[1]EDiSt code is available at https://github.com/vtsynergy/EDiSt

- An evaluation of EDiSt's scalability, showing that by scaling out to 64 compute nodes, EDiSt achieves up to 44.0× speedup over shared memory parallel SBP and a 23.8× speedup over divide-and-conquer distributed SBP.

## II. BACKGROUND AND RELATED WORK

In this section, we provide some background on stochastic blockmodels, the stochastic block partitioning algorithm, and the state-of-the-art in distributed stochastic block partitioning.

### A. Stochastic Blockmodels

Stochastic blockmodels (SBMs) [7] are a class of generative models that describe the structure of a graph based on its community structure. They can be used to either generate graphs with a specified community structure or to infer the community structure of a specified graph.

Typically, a stochastic blockmodel is represented by a matrix $M$ of size $C \times C$, where $C$ refers to the number of communities present in the model. Every entry $M_{a,b}$ of the blockmodel matrix corresponds to the number of edges between (or if the blockmodel is not microcanonical, the probability of edges forming between) two communities $a$ and $b$.

A quality function is used to fit blockmodels to a given graph when using them to perform community detection. One such function is the log-likelihood of the graph $G$ given the blockmodel $B$, $L(G|B)$. The log-likelihood function varies between the different variants of SBMs. In this paper, we focus on the degree-corrected SBM (DCSBM), which accounts for differences in degree distribution between communities in a graph. The log-likelihood for the DCSBM is given by the following equation [6], [11]:

$$L(G|B) = \sum_{i,j} B_{i,j} \log \left( \frac{B_{i,j}}{d_i^{out} d_j^{in}} \right), \qquad (1)$$

where $B_{i,j}$ is the number of edges between communities $i$ and $j$, and $d_i^{out}$ and $d_j^{in}$ are the out-degree of community $i$ and the in-degree of community $j$, respectively, for a directed graph.

However, the log-likelihood function is unsuitable for community detection where the number of communities is not known apriori. This is because $L(G|B)$ will be maximized when the number of communities $C$ is equal to the number of vertices $V$. To overcome this limitation, when the optimal number of communities needs to be inferred alongside the optimal vertex-to-community assignment, the description length metric, $DL$, is used instead of $L(G|B)$. For a directed graph, $DL$ is given by the following equation [11], [16]:

$$DL = Eh \left( \frac{C^2}{E} \right) + V \log C - L(G|B), \qquad (2)$$

where $E$ is the number of edges in the graph, $C$ is the number of communities in the graph, $h(x) = (1 + x) \log 1 + x - x \log x$, $V$ is the number of vertices in the graph and $L(G|B)$ is given by Equation (1). Unlike $L(G|B)$, $DL$ is minimized when used to infer the community structure of a graph.

## B. Stochastic Block Partitioning

Stochastic block partitioning (SBP) [6], [8], [11] is a community detection algorithm based on inference over the degree-corrected stochastic blockmodel (DCSBM). It minimizes the description length of the DCSBM, as shown in Equation (2), using Markov chain Monte Carlo (MCMC) techniques.

This optimization is iterative, agglomerative, and executed in two alternating phases: the block merge phase and the MCMC phase. In the MCMC phase, described in Algorithm 2, the inherently sequential Metropolis-Hastings algorithm [17] is used to move individual vertices from one community to another, based on the change in the description length of the DCSBM. In the block merge phase, described in Algorithm 1, entire communities (or blocks) are merged together, reducing the likelihood of the MCMC process getting stuck in a local minimum. The algorithm's execution is summarized in Fig. 1.

To allow the algorithm to automatically find the optimal number of communities, a golden ratio search is used. In this search algorithm, up to three versions of the blockmodel are stored in decreasing order of number of communities. So long as all three blockmodels are also in decreasing order of description length, the next phase of the algorithm will start with the blockmodel with the smallest number of communities and proceed with the block merge phase. If, however, the subsequent blockmodel results in an increased description length, then the golden ratio criterion is met, and the optimal number of communities is within the range specified by the three stored blockmodels.

A parallel formulation of SBP was proposed in [13]. This formulation replaced the Metropolis-Hastings portion of the algorithm with a hybrid algorithm that processes informative, high-degree vertices sequentially and the less informative low-degree vertices in parallel via an adaptation of asynchronous Gibbs sampling [18].

---

**Algorithm 1:** Block Merge Phase

**Data:** Graph $G$, Blockmodel $B$, int $x$
**Result:** Updated Blockmodel $B$

1   initialize best_merges container;
2   **for** *community* $c \in B$ **do in parallel**
3     // x set to 10 as per reference implementation
     **repeat** $x$ **times**
4       Propose a new community $c'$ to merge with $c$;
5       Calculate $\Delta DL$ when $c$ is merged with $c'$;
6       **if** $\Delta DL$ *is best obtained so far for* $c$ **then**
7        Store $(c, c', \Delta DL)$ in best_merges;
8       **end**
9     **end**
10   **end**
11   sort best_merges on $\Delta DL$;
12   **repeat**
13     $c, c', \Delta DL$ = best_merges.pop();
14     Merge $c$ into $c'$;
15   **until** *number of communities is halved*;

---

**Algorithm 2:** MCMC Phase

**Data:** Graph $G$, Blockmodel $B$, double $t$, int $x$
**Result:** Updated Blockmodel $B$

1   compute DL of $B$;
2   **repeat**
3     **foreach** *vertex* $v \in G$ **do**
4       propose new community $c$ for $v$;
5       compute $\Delta DL$ for proposed move;
6       compute Metropolis-Hastings ratio from $\Delta DL$;
7       **if** *move is accepted* **then**
8        move $v$ to $c$ and update $B$;
9       **end**
10     **end**
11   compute DL of $B$;
12   **until** $\Delta DL < t \times DL$ *or* $x$ *times*;

---

## C. Divide-and-Conquer SBP

The data access patterns of SBP make distributing the algorithm a non-trivial task. For every proposed change in community membership, the algorithm needs access to at least two rows *and* two columns of the SBM matrix. Thus, a row- or column-wise distribution of the blockmodel would lead to all-to-one communication for every proposed change in community membership. Moreover, any accepted changes in community membership (and the corresponding changes to the blockmodel rows and columns) would need to be broadcast to every other worker. A "traditional" distribution of the algorithm would therefore be ineffective due to excessive amounts of communication.

To the best of our knowledge, the only published distributed SBP algorithm is the MPI-based divide-and-conquer (DC-SBP) algorithm of Uppal, Swope, and Huang [15], developed as part of the MIT/Amazon/IEEE Graph Challenge [11]. DC-SBP divides the graph into $n$ subgraphs, where $n$ is the number of MPI ranks/tasks. Each rank then runs the SBP algorithm on its subgraph independently until the golden ratio criterion is reached. The resulting community memberships are then sent to the root rank, where they are combined. This combination happens in two steps.

In the first step, community memberships from successive subgraph pairs are iteratively combined, such that each community from one subgraph is merged into a community from the other subgraph. The merges are selected based on the best potential change in DL. This is repeated until the number of subgraphs is reduced to a threshold $t$, which was chosen as four by the authors. This allows the algorithm to potentially recover if some subgraphs do not contain the same communities.

In the second step, the remaining community memberships are merged to form the community memberships for the entire graph. SBP then continues on the whole graph using the root rank, thus fine-tuning the merged results and allowing the algorithm to find the optimal number of communities.

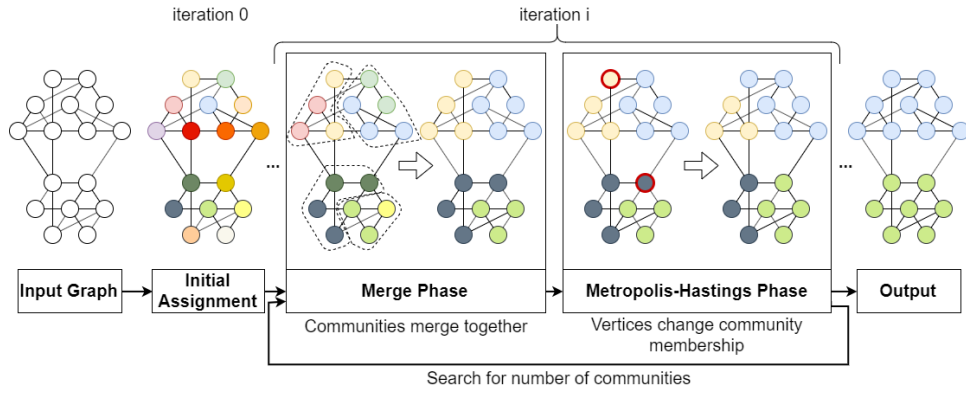The pseudocode for DC-SBP is given in Alg. 3 while

Fig. 1. Snapshots of a graph at various stages of the stochastic block partitioning algorithm.

the actual code is available at https://github.com/iHeartGraph/GraphChallenge. Their implementation is written in Python using NumPy [19] for array operations and the mpi4py library [20] for distributed computation. Since Python is an interpreted language, this Python implementation can be significantly sped up by translating it to C++, which we do in Section III-A.

---

**Algorithm 3:** Divide-and-Conquer SBP

**Data:** Graph $G$, MPI rank $r$
**Result:** Blockmodel $B$

1 subgraph $G^r$ = round robin sample from $G$ based on $r$;
2 partial blockmodel $B^r$ = create initial blockmodel from $G^r$;
3 $B^r$ = SBP($G^r$, $B^r$);
4 partial results $R$ = list($B^r$);
5 **if** $r == 0$ **then**
6    **foreach** *rank* $r', r' \neq 0$ **do**
7      partial result $B^{r'}$ = MPI_Recv($r'$);
8      append $B^{r'}$ to $R$
9    **end**
10 **else**
11    MPI_Send $B^r$ to rank 0;
12    return;
13 **end**
14 **repeat**
15    $R'$ = list();
16    **foreach** *successive* $B^{r1}, B^{r2} \in R$ **do**
17      $B'$ = merge $B^{r2}$ communities into $B^{r1}$ communities;
18      append $B'$ to $R'$
19    **end**
20    $R = R'$;
21 **until** $R.length \leq 4$;
22 intermediate blockmodel $B'$ = merge partial results in $R$;
23 return SBP($B'$);

---

The disconnectedness between the subgraphs in DC-SBP

results in minimal communication between MPI ranks/tasks, which theoretically allows the algorithm to efficiently scale to a large number of nodes and neatly solves the problem of how to distribute the blockmodel matrix. However, it also creates convergence issues by breaking several computational dependencies in the graph. Therefore, in practice, scaling the algorithm to a large number of MPI tasks leads to severe accuracy degradation (see SectionV-B).

Additionally, the fine-tuning phase happens on a single computational node. These fine-tuning SBP iterations are faster than the initial ones due to a greatly decreased number of communities (assuming that the number of communities is a small fraction of the number of vertices, which is generally true in practice) and a decrease in the number of vertices that change community membership, which leads to fewer blockmodel updates being performed. However, on large graphs, they can still present a significant performance bottleneck.

## III. METHOD

Here we describe our baseline DC-SBP implementation and our exact distributed stochastic block partitioning algorithm.

### A. C++ Divide-and-Conquer SBP Implementation

To speed up the divide-and-conquer SBP implementation, we first translate the Python implementation to C++ and use MPI for communication between nodes. We then optimize the translated implementation for faster execution on sparse graphs. Some of the optimizations implemented include

- storing the blockmodel matrix as a vector of hashmap objects for fast indexing *and* modification of the matrix;
- storing the transpose of the blockmodel matrix for fast access along both rows and columns at the expense of additional memory usage;
- using a sparse vector of changes to the blockmodel to compute changes in description length and to update the blockmodel matrix when an MCMC move is accepted;
- using a disjoint-set data structure to keep track of community merges during the block merge phase of SBP, which speeds up the block merge phase of the algorithm.

While we can speed up the gathering of partial results to the root MPI rank using collective operations, this is not necessary since the gather operation only executes once and does not consume a significant amount of time.

To parallelize the computation within an MPI rank, we use our hybrid SBP [13] algorithm implemented using OpenMP.

### B. Exact Distributed SBP

The main difference between the DC-SBP algorithm and our exact distributed approach lies in the inter-subgraph connectivity. In DC-SBP, the subgraphs are disconnected, and an MPI rank working on subgraph A has no knowledge of the vertices or the communities in subgraph B. As such, the more ranks (and subgraphs) there are, the less information a rank has access to and the higher the chances that the SBP algorithm fails to converge. The upside of this lack of connectivity is that processing each subgraph requires much less memory and is much faster, both due to the super-linear runtime of SBP and the minimal inter-node communication.

In our exact distributed approach, we allow each rank to have knowledge of the vertices and communities present in the other ranks. Each rank stores the blockmodel for the entire graph but is responsible for the computation of only a portion of the communities or vertices, depending on the phase of the algorithm. Since communicating every change to the blockmodel is impractical due to the communication burden this would impose, we allow the ranks to synchronize their blockmodels at the end of every block merge phase and after each MCMC iteration.

In the block merge phase, each rank is responsible for computing the merge proposals and corresponding changes in description length for a disjoint set of communities. Once these computations are done, the ranks communicate the merge proposal with the best (most negative) change in description length for each of the communities they are responsible for, to all the other ranks using MPI all-to-all communication primitives. Each rank then selects the best merges according to their computed change in description length and updates its blockmodel accordingly. The pseudocode for this phase is shown in Algorithm 4.

In the MCMC phase, each rank is responsible for computing proposals to change community memberships and the corresponding changes in description length for a disjoint set of vertices. Each rank makes a pass over the vertices assigned to it, updating its local copy of the blockmodel, as needed, and storing the move in a vector. At the end of the pass, the ranks exchange the accepted moves using MPI all-to-all communication primitives. Then, each rank updates its local copy of the blockmodel by performing the moves received from all other ranks. The pseudocode for this phase is shown in Algorithm 5. Note that for consistency, the pseudocode shown is for the sequential, Metropolis-Hastings-based MCMC phase. However, the differences between the distributed hybrid MCMC phase used in this work and the distributed Metropolis-Hastings MCMC phase are minimal.

---

**Algorithm 4:** Block Merge Phase in EDIST

**Data:** Graph $G$, Blockmodel $B$, int $x$, MPI rank $r$
**Result:** Updated Blockmodel $B$

1. N = MPI_Comm_size(MPI_COMM_WORLD);
2. initialize best_merges container;
3. **for** *community $c \in B$* **do in parallel**
4.      **if** $c \bmod N \neq r$ **then**
5.         continue;
6.      **end**
7.      **repeat** $x$ **times**
8.         Propose a new community $c'$ to merge with $c$;
9.         Calculate $\Delta DL$ when $c$ is merged with $c'$;
10.        **if** *$\Delta DL$ is best obtained so far for $c$* **then**
11.           Store $c'$ and $\Delta DL$ for $c$ in best_merges;
12.        **end**
13.     **end**
14. **end**
15. MPI_Allgather(best_merges);
16. sort best_merges on $\Delta DL$;
17. **repeat**
18.     $c$, $c'$ = best_merges.pop();
19.     Merge $c$ into $c'$;
20. **until** *number of communities is halved*;

---

**Algorithm 5:** MCMC Phase in EDIST

**Data:** Graph $G$, Blockmodel $B$, double $t$, int $x$, list $V'$ of vertices this rank is responsible for
**Result:** Updated Blockmodel $B$

1. compute DL of $B$;
2. **repeat**
3.      initialize accepted_merges container;
4.      **foreach** *vertex $v \in G$* **do**
5.         **if** $v \notin V'$ **then**
6.            continue;
7.         **end**
8.         propose new community $c$ for $v$;
9.         compute $\Delta DL$ for proposed move;
10.        compute Metropolis-Hastings ratio from $\Delta DL$;
11.        **if** *move is accepted* **then**
12.           move $v$ to $c$ and update $B$;
13.           store $v$ and $c$ in accepted_merges;
14.        **end**
15.     **end**
16.     MPI_Allgather(accepted_merges);
17.     **foreach** *$v$ and $c$ pair in accepted_merges* **do**
18.        **if** *vertex $v$ is not in community $c$* **then**
19.           move $v$ to $c$ and update $B$;
20.        **end**
21.     **end**
22.     compute DL of $B$;
23. **until** *$\Delta DL < t \times DL$ or $x$ times*;

To maintain load balance in the MCMC phase, we adopt a method similar to the sorting-based blocking algorithm described in [21]. We first sort the vertices according to vertex degree. Then, assuming there are $n$ ranks, rank $r$ gets assigned the set of vertices $(r, 2n - r, 2n + r, 4n - r, 4n + r, 6n - r, ...)$. This has the effect of breaking the sorted set of vertices in chunks of $2n$ and then assigning to each rank the vertices with the $r$th highest and $r$th lowest degrees. On the 200k-hard graph described in Table II, we found that with 32 MPI ranks the imbalance time [22] for the MCMC phase of EDiSt is about 1.75 seconds or 2.2% of the total MCMC runtime. In other words, optimal load balancing for that run would only provide a maximum additional speedup of $1.02\times$.

The synchronization of the blockmodels between ranks and the fact that each rank keeps track of the entire blockmodel means that the exact distributed SBP approach is likely to be slower and require more memory per rank than DC-SBP. At the same time, these weaknesses allow it to scale to a much higher number of ranks before accuracy degradation can be expected to set in (as $n$ approaches $V$, EDiSt becomes equivalent to asynchronous Gibbs, which has previously been shown to degrade performance on some synthetic graphs [13]). On graphs with a particularly sparse dependency distribution, it is theoretically possible to scale the approach to $V$ MPI ranks without any accuracy degradation.

## IV. EXPERIMENTAL SETUP

In this section, we describe the datasets and hardware used to evaluate DC-SBP and EDiSt.

### A. Synthetic Datasets

We use the datasets published in the MIT/Amazon/IEEE Graph Challenge [11] to compare the results of our approach with those presented in [15]. These graphs were generated using the 'graph-tool' [23] Python library by generating a blockmodel with the desired characteristics and then perturbing a random graph until it matches these characteristics as closely as possible. The selected graphs are summarized in Table II. The graphs labeled as 'easy' correspond to those with a low block overlap and low block size variation, and those labeled as 'hard' correspond to those with a high block overlap and high block size variation.

When testing the divide-and-conquer approach, we noticed significant differences in how well the algorithm retains accuracy as the number of nodes increases based on the graph structure. On the Graph Challenge [11] graphs, the divide-and-conquer approach maintained accuracy until between 8 and 16 MPI ranks; but on the web-graph-like graphs used in [13], the divide-and-conquer approach sometimes failed to maintain accuracy even with two MPI ranks. This is despite the fact that both sets of graphs were generated using a similar approach, using the blockmodel-based generator from the 'graph-tool' [23] Python library. To determine the cause of this disparity, we identified the following differences between the two sets of graphs:

- Number of communities: the Graph Challenge graphs had a significantly smaller ratio of communities to vertices.
- Degree sequence duplication: the 'graph-tool' graph generator requires a sequence of vertex degrees, describing the graph's degree distribution, to be passed to its generating function. In the graph-tool, a single sequence was used for both the in-degrees and out-degrees of the graph's vertices, essentially ensuring that the minimum total degree of a vertex is equal to twice the smallest in-degree. In the web-graph-like graphs, a total degree sequence is generated, and its values are then randomly split between the in-degree and out-degree sequences, thus allowing the generator to output vertices with a total degree of one.
- Truncation of degree distribution: the Graph Challenge graphs truncate the degree distribution to between 10 and 100 (which effectively becomes 20 and 200 when coupled with the degree sequence duplication described above). The web-graph-like graphs have a much wider degree distribution, with the minimum degree set to one and the maximum degree set to a fraction of the number of vertices in the graph.

We then generate a set of 16 synthetic graphs that form an exhaustive parameter search study of these differences. These graphs are described in Table III. For reference, the Graph Challenge datasets are closest in structure to the TTT33 graph, while the web-graph-like graphs are closest in structure to the FFF150 graph.

We also generate large, synthetic graph datasets for testing the scalability of distributed community detection. These datasets, which range from 11 to 300 million edges, are summarized in Table IV.

TABLE IV
SYNTHETIC GRAPHS USED IN SCALING STUDY

| ID | Number of Communities | Number of Vertices | Number of Edges |
|----|----------------------|--------------------|-----------------|
| 1M | 1075 | 1051218 | 11056834 |
| 2M | 1521 | 2103554 | 23987218 |
| 4M | 2151 | 4221264 | 53175026 |

To ensure the rigor of our experimental evaluation of DC-SBP and EDiSt, we generate all synthetic graphs to have a complex community structure in accordance with the high overlap, high block size variation graphs used in the Graph Challenge [11]. That is, the ratio of intra-community to inter-community edges is roughly 2, and the approximate sizes of the communities are drawn from a random Dirichlet distribution with $\alpha = 2$.

### B. Real-world datasets

We also test our approach on real-world data from a variety of domains. The five graphs outlined in Table V are graphs from the Stanford Large Network Dataset Collection [24] and the Laboratory for Web Algorithmics dataset collection [25]–[27], obtained in Matrix Market format via the SuiteSparse

TABLE II
GRAPH CHALLENGE DATASETS

| ID | Number of Vertices | Number of Edges | Community Overlap | Community Size Variation | Number of Communities |
|---|---|---|---|---|---|
| 20K-easy | 20,000 | 473914 | low | low | 32 |
| 20k-hard | 20,000 | 473329 | high | high | 32 |
| 50K-easy | 50,000 | 1183975 | low | low | 44 |
| 50k-hard | 50,000 | 1187682 | high | high | 44 |
| 200k-easy | 200,000 | 4750333 | low | low | 71 |
| 200k-hard | 200,000 | 4754406 | high | high | 71 |

TABLE III
SYNTHETIC GRAPHS USED IN EXHAUSTIVE PARAMETER SEARCH STUDY

| ID | Truncated Min Degree | Truncated Max Degree | Duplicated Degree Sequence | Number of Communities | Number of Vertices | Number of Edges | Average Degree |
|---|---|---|---|---|---|---|---|
| TTT33 | True | True | True | 33 | 22599 | 899283 | 39.8 |
| TTT150 | True | True | True | 150 | 22599 | 826861 | 36.6 |
| TTF33 | True | True | False | 33 | 22599 | 452232 | 20.0 |
| TTF150 | True | True | False | 150 | 22599 | 421317 | 18.6 |
| TFT33 | True | False | True | 33 | 22599 | 1059970 | 46.9 |
| TFT150 | True | False | True | 150 | 22599 | 912644 | 40.4 |
| TFF33 | True | False | False | 33 | 22599 | 540410 | 23.9 |
| TFF150 | True | False | False | 150 | 22598 | 471071 | 20.8 |
| FTT33 | False | True | True | 33 | 21896 | 79683 | 3.6 |
| FTT150 | False | True | True | 150 | 22036 | 78226 | 3.5 |
| FTF33 | False | True | False | 33 | 19220 | 39719 | 2.1 |
| FTF150 | False | True | False | 150 | 19221 | 38408 | 2.0 |
| FFT33 | False | False | True | 33 | 22157 | 83939 | 3.8 |
| FFT150 | False | False | True | 150 | 21958 | 81298 | 3.7 |
| FFF33 | False | False | False | 33 | 19516 | 41378 | 2.1 |
| FFF150 | False | False | False | 150 | 19358 | 40835 | 2.1 |

Matrix Collection [28]. These graphs range from 3.4 to 194 million edges in size and do not have robust, non-overlapping ground-truth communities.

TABLE V
REAL-WORLD GRAPHS USED IN SCALING STUDY

| Graph ID | Description | Number of Vertices | Number of Edges |
|---|---|---|---|
| Amazon | Amazon co-purchasing graph | 403394 | 3387388 |
| Berk-Stan | Web graph containing hyperlinks | 685230 | 7600595 |
| Twitter | Twitter social network graph | 456626 | 14855842 |
| Patents | Citation graph in US patents | 3774768 | 16418948 |
| Live-Journal | LiveJournal social network graph | 4847571 | 68993773 |
| In-dochina | Web crawl of country domains | 7414866 | 194109311 |

### C. Hardware

All our strong-scaling experiments are run on the base compute nodes of the Virginia Tech TinkerCliffs cluster. TinkerCliffs contains 308 base compute nodes, each equipped with 128-core AMD EPYC 7702 chips and having 256 GB of memory. The 128 cores are arranged in eight NUMA nodes with 16 cores each, and the interconnect used is HDR-100 IB. Though the total number of base compute nodes is 308, the maximum number of nodes allowed in any slurm job is 64. Hence, our experiments are limited to 64 compute nodes.

Our smaller experiments were run on the Dell nodes of the Virginia Tech Infer cluster. Infer contains 40 Dell nodes with 28 cores per node, 512Gb of memory each and uses an Ethernet interconnect.

## V. RESULTS

Here we present the results of our evaluation of DC-SBP and SBP. We show that our C++ DC-SBP implementation is just as accurate as the original Python implementation while being faster. We illustrate the two failure modes of DC-SBP and show that EDiSt does *not* exhibit these failure modes. Finally, we show that by leveraging its improved scalability, EDiSt provides faster runtimes and higher accuracy than DC-SBP on both synthetic and real-world graphs.

### A. Accuracy of our C++ DC-SBP Implementation

To ascertain that our C++ DC-SBP implementation is just as accurate as the original Python implementation, we compare the normalized mutual information (NMI) results obtained at eight MPI ranks with the original Python DC-SBP implementation and our C++ DC-SBP implementation on the Graph Challenge graphs (similar to the ones for which results were reported in [15]) on the Infer cluster. The results, summarized in Table V-A show that the NMI obtained with our C++ implementation matches or exceeds the NMI obtained with the Python implementation on all three graphs.

TABLE VI
COMPARISON BETWEEN PYTHON AND C++ DC-SBP
IMPLEMENTATIONS

| Graph ID | Python | | C++ | |
|---|---|---|---|---|
| | NMI[1] | Runtime (s) | NMI[1] | Runtime (s) |
| 20k-easy | 0.98 | 171 | 1.00 | 26 |
| 20k-hard | 0.82 | 163 | 0.86 | 30 |
| 50k-easy | 0.96 | 441 | 1.00 | 100 |
| 50k-hard | 0.72 | 379 | 0.84 | 178 |
| 200k-easy | 0.93 | 7641 | 1.00 | 604 |
| 200k-hard | 0.81 | 7244 | 0.81 | 479 |

[1] NMI = normalized mutual information.

The improved runtime performance is due to our optimizations and the use of a compiled language. The slight improvement in NMI is most likely due to our use of the Hybrid SBP algorithm for parallelizing MCMC movements within a node, compared to the batch-based parallelism employed in the original Python implementation.

### B. Exhaustive Parameter Search Study

We run DC-SBP with varying numbers of compute nodes on the exhaustive parameter search study graphs described in III and record the resulting NMI. The results are summarized in Table VII (left).

These results illustrate the two conditions where DC-SBP suffers from convergence issues. The first condition occurs when the number of compute nodes (or MPI tasks) is greater than or equal to 16. The second condition occurs when the degree distribution is *not* truncated on the minimum degree side (i.e., the minimum vertex degree is one or two). This is because this parameter has the biggest effect on the density of the graph, and the resulting graphs are significantly more sparse than the graphs with a truncated degree distribution. This suggests that DC-SBP works much better on denser graphs, and could explain why DC-SBP maintains NMI on TFT33, the densest of these graphs, at 16 compute nodes.
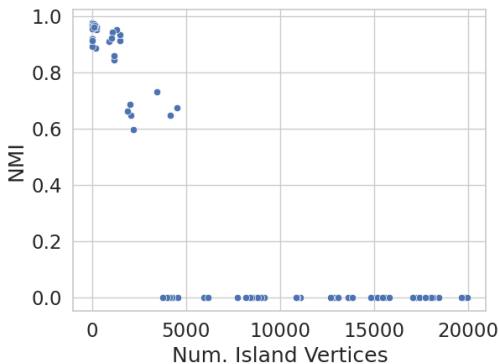


Fig. 2. Relationship between the number of island vertices induced by the data distribution and the resulting NMI.

We attribute this to the number of island vertices induced by the data distribution method in DC-SBP. This is corroborated

by Figure 2, which shows the relationship between the number of island vertices and the NMI obtained on the results in Table VII above. As the number of island vertices increases, the NMI decreases. DC-SBP appears to be robust up to a relatively high number of island vertices of around 10%, but NMI drops off after that and rests at zero beyond 20%. Tellingly, on the sparser graphs, and with a high number of compute nodes, the data distribution scheme results in upwards of 50% island vertices.

We repeat the exhaustive parameter search study using EDiSt on the same set of graphs and record the results in Table VII (right). Our results demonstrate that EDiSt converges well even when the number of compute nodes is high, and the graphs are sparse due to a power law degree distribution with the minimum degree being one.

### C. Scalability Analysis on Synthetic Graphs

In this subsection, we discuss the scalability of EDiSt on synthetic graphs and compare the results to those obtained with DC-SBP.

*1) Scalability on a Single Node:* The hybrid MCMC method described in [13] alternates between sequential and parallel MCMC execution. This leads to extended periods of low CPU utilization where only one thread is running. In such cases, running EDiSt on multiple MPI tasks on the same node can improve SBP runtime, provided the node has enough memory and the total number of tasks is significantly smaller than the number of high-degree vertices in the graph (in this case, the hybrid parallel MCMC algorithm would devolve into asynchronous Gibbs, which could reduce accuracy on certain graphs).
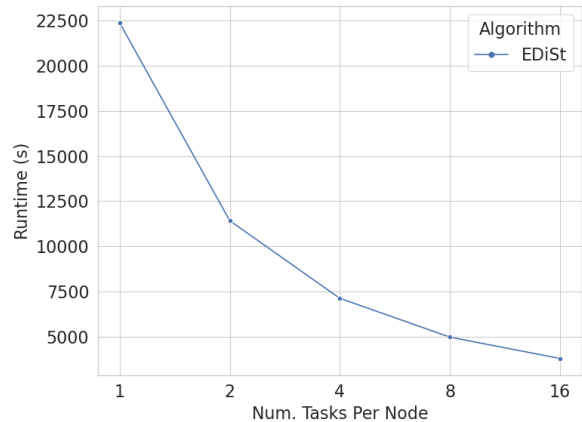


Fig. 3. EDiSt runtime with multiple MPI tasks per compute node.

In Figure 3, we showcase this increase in speedup by running EDiSt on the 1M graph described in Table IV on a single node, and increasing the number of MPI tasks until we run out of memory.

Our results indicate that there is a runtime benefit to running multiple EDiSt MPI tasks per node, with a speedup of $9\times$ with 16 MPI tasks per node. In all proceeding sections, we run

TABLE VII
NMI RESULTS ON EXHAUSTIVE PARAMETER SEARCH GRAPHS

| Graph ID | NMI with DC-SBP at Number of Nodes | | | | | | | Graph ID | NMI with EDiSt at Number of Nodes | | | | | | |
|---|---|---|---|---|---|---|---|---|---|---|---|---|---|---|---|
| | Baseline (1) | 2 | 4 | 8 | 16 | 32 | 64 | | Baseline (1) | 2 | 4 | 8 | 16 | 32 | 64 |
| TTT33 | 0.92 | 0.96 | 0.89 | 0.90 | 0.87 | 0.00 | 0.00 | TTT33 | 0.92 | 0.88 | 0.94 | 0.93 | 0.95 | 0.95 | 0.94 |
| TTT150 | 0.97 | 0.97 | 0.97 | 0.96 | 0.88 | 0.00 | 0.00 | TTT150 | 0.97 | 0.97 | 0.97 | 0.97 | 0.97 | 0.97 | 0.97 |
| TTF33 | 0.96 | 0.89 | 0.95 | 0.95 | 0.00 | 0.00 | 0.00 | TTF33 | 0.96 | 0.89 | 0.96 | 0.96 | 0.95 | 0.96 | 0.96 |
| TTF150 | 0.95 | 0.96 | 0.96 | 0.93 | 0.67 | 0.00 | 0.00 | TTF150 | 0.95 | 0.95 | 0.95 | 0.96 | 0.97 | 0.97 | 0.95 |
| TFT33 | 0.97 | 0.97 | 0.97 | 0.91 | 0.96 | 0.73 | 0.00 | TFT33 | 0.97 | 0.96 | 0.98 | 0.98 | 0.97 | 0.96 | 0.96 |
| TFT150 | 0.97 | 0.97 | 0.97 | 0.96 | 0.80 | 0.00 | 0.00 | TFT150 | 0.97 | 0.97 | 0.97 | 0.97 | 0.97 | 0.97 | 0.97 |
| TFF33 | 0.97 | 0.92 | 0.89 | 0.97 | 0.65 | 0.00 | 0.00 | TFF33 | 0.97 | 0.96 | 0.96 | 0.97 | 0.97 | 0.96 | 0.96 |
| TFF150 | 0.96 | 0.96 | 0.96 | 0.93 | 0.00 | 0.00 | 0.00 | TFF150 | 0.96 | 0.95 | 0.97 | 0.96 | 0.95 | 0.95 | 0.95 |
| FTT33 | 0.66 | 0.53 | 0.00 | 0.00 | 0.00 | 0.00 | 0.00 | FTT33 | 0.66 | 0.66 | 0.66 | 0.67 | 0.67 | 0.65 | 0.66 |
| FTT150 | 0.72 | 0.59 | 0.00 | 0.00 | 0.00 | 0.00 | 0.00 | FTT150 | 0.72 | 0.72 | 0.72 | 0.73 | 0.72 | 0.70 | 0.72 |
| FTF33 | 0.38 | 0.00 | 0.00 | 0.00 | 0.00 | 0.00 | 0.00 | FTF33 | 0.38 | 0.38 | 0.38 | 0.35 | 0.36 | 0.34 | 0.38 |
| FTF150 | 0.48 | 0.00 | 0.00 | 0.00 | 0.00 | 0.00 | 0.00 | FTF150 | 0.48 | 0.42 | 0.48 | 0.44 | 0.49 | 0.39 | 0.48 |
| FFT33 | 0.74 | 0.66 | 0.00 | 0.00 | 0.00 | 0.00 | 0.00 | FFT33 | 0.74 | 0.75 | 0.74 | 0.74 | 0.75 | 0.75 | 0.73 |
| FFT150 | 0.72 | 0.69 | 0.00 | 0.00 | 0.00 | 0.00 | 0.00 | FFT150 | 0.72 | 0.71 | 0.72 | 0.72 | 0.72 | 0.75 | 0.72 |
| FFF33 | 0.34 | 0.00 | 0.00 | 0.00 | 0.00 | 0.00 | 0.00 | FFF33 | 0.34 | 0.35 | 0.38 | 0.36 | 0.38 | 0.38 | 0.40 |
| FFF150 | 0.48 | 0.00 | 0.00 | 0.00 | 0.00 | 0.00 | 0.00 | FFF150 | 0.48 | 0.51 | 0.53 | 0.51 | 0.51 | 0.52 | 0.53 |

EDiSt with four MPI tasks per node (we run out of memory when attempting more tasks per node with larger graph sizes). We do not do the same for DC-SBP, because the convergence issues observed when the number of MPI ranks is increased make such a solution impractical for that algorithm.

*2) Strong Scaling:* We run EDiSt on the synthetic scaling graphs we describe in Table IV and measure the resulting NMI and Runtime. Figure 4 shows the runtime and NMI results of EDiSt as the number of nodes increases from 1 to 64.
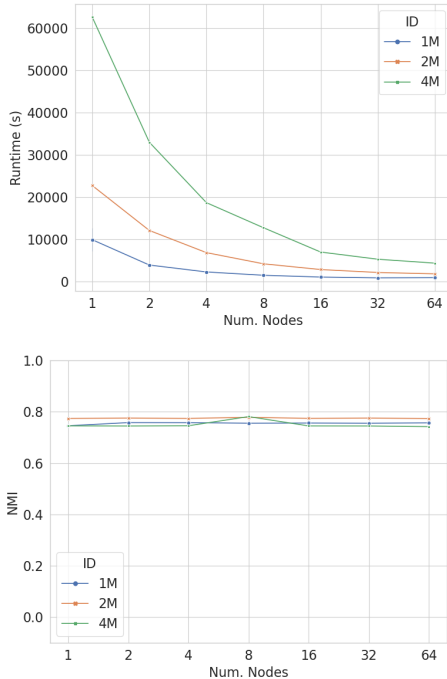


Fig. 4. EDiSt strong scaling (top) and NMI (bottom) results on synthetic graphs.

These results confirm that EDiSt maintains result quality both at high numbers of MPI tasks and on sparse graphs.

Given that we run EDiSt with 4 MPI tasks per node, EDiSt is therefore usable on at least $16\times$ more MPI tasks than DC-SBP. Though the runtimes do start to plateau, the level-off point increases as the graph size increases, suggesting that up to 64 nodes, the runtime benefits of EDiSt will scale with the graph size.

*3) Comparison with DC-SBP:* We then compare the speedups obtained with EDiSt to those obtained with DC-SBP. In the case of DC-SBP, for each graph, we select the runtime at the highest number of MPI tasks at which DC-SBP maintains NMI with the single-node shared-memory baseline. The results are shown in Figure 5.
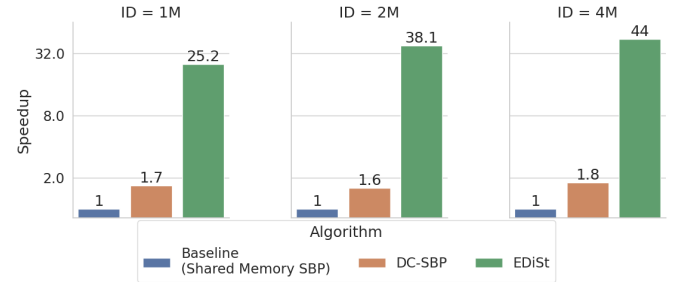


Fig. 5. Comparison of the best speedup achieved with DC-SBP and EDiSt on the three synthetic scaling graphs.

These results show that EDiSt on 64 compute nodes is up to $44.0\times$ faster than single node shared memory SBP, and up to $23.8\times$ faster than the best-performing DC-SBP run that did not suffer from convergence issues.

### D. Real-World Graphs Results

Finally, we run both DC-SBP and EDiSt on the real-world datasets described in Table V. Due to memory restrictions, when running EDiSt on the Indochina graph, we use two MPI tasks per node instead of four. Because real-world graphs do not have known ground truth communities, we measure
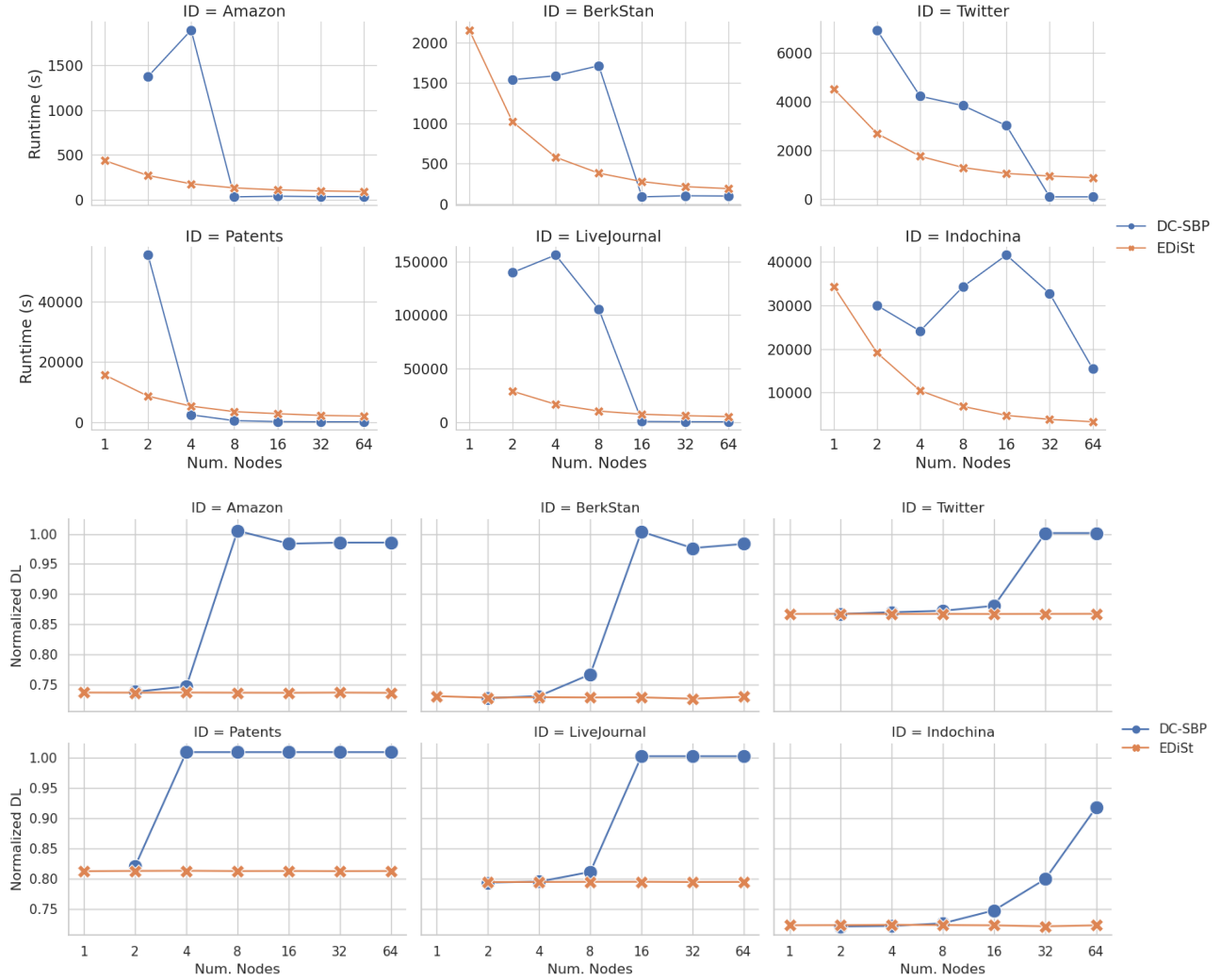
Fig. 6. EDiSt vs DC-SBP strong scaling (top) and accuracy as measured by Normalized DL (bottom, lower is better) results on real-world graphs. The single-node EDiSt run on LiveJournal was not completed due to excessive runtime.

accuracy using the normalized description length ($DL^{norm}$) metric [13], which is given by the equation: $DL^{norm} = \frac{DL}{DL^{null}}$, where $DL$ refers to the description length of the blockmodel returned by either algorithm and $DL^{null}$ refers to the description length of a null blockmodel where all vertices are assigned to the same singular community.

The $DL^{norm}$ and strong scaling results obtained are summarized in Figure 6. EDiSt is up to $26.8\times$ faster than DC-SBP on these graphs because DC-SBP usually produces meaningful results on only 2-8 subgraphs. On the Twitter and Indochina graphs, which have the highest average degrees, DC-SBP maintains accuracy reasonably well up to 16 subgraphs. As such, EDiSt's speedup over DC-SBP on the Twitter and Indochina graphs is only $3.4\times$ and $7.3\times$, respectively. Therefore, these results corroborate our findings on synthetic graphs.

In addition to measuring runtime, we profile the execution of EDiSt on the LiveJournal graph on 64 compute nodes (256 MPI ranks) using the mpiP software. The profiling results showed that MPI calls took up 6.7% of EDiSt's total runtime, with a total of 100.2GB of packets being communicated between the MPI ranks. Thus, at this scale, further algorithmic refinements of SBP are more likely to significantly speed up the algorithm than optimizing communication patterns.

### E. Discussion

Our results show that DC-SBP has convergence issues on sufficiently sparse graphs, and when the number of compute nodes (and therefore, distinct subgraphs) is 16 or higher. Thus, its applicability is limited to dense graphs on small clusters. On the other hand, the exact distributed stochastic block partitioning (EDiSt) algorithm converges in both of these scenarios, making it applicable in a much wider variety of situations. In addition to this, the single-node partial result combination in DC-SBP leads to severe bottlenecks on larger graphs with more communities, to the point where the theoretically slower EDiSt outperforms it on the same number of nodes.

However, DC-SBP does have one major advantage over EDiSt - it incorporates data distribution. With the advent of web-scale graphs, which contain on the order of billions of edges, data distribution is becoming more and more important for large graph processing. However, given the current state of the SBP algorithm, we argue that runtime is a bigger bottleneck than memory usage. For example, the 69 million edge LiveJournal graph takes over an hour to process on 64 nodes. More importantly, we were able to load in a 300M edge synthetic graph on the tinkercliffs cluster, but could not complete its processing within eight hours on 64 nodes. Additionally, data reduction techniques like sampling, which have been shown to preserve community structure in graphs [12], [29], [30], are a promising means of reducing the memory footprint of graphs that do not fit in memory.

It should be noted that even on 64 nodes, EDiSt is slower than various shared memory implementations of non-inferential community detection algorithms. As discussed in [9], inference-based methods such as SBP are preferred over other heuristics when performing data analysis tasks, where it is important to explain the nature of the communities, as these methods are less prone to overfitting and can distinguish between random graphs and graphs with an inherent community structure. In tasks such as load balancing, where the number of between-community edges needs to be minimized but there is no need to explain why or how these communities came about, the faster heuristics are likely to be preferred over SBP.

## VI. CONCLUSION

Community detection is an important graph analytics task with applications in a wide variety of fields, from bioinformatics to social media analytics. Due to the growth in the size of modern graph datasets, sequential community detection algorithms are no longer practical for many real-world scenarios. This presents a problem for relatively slow and hard-to-parallelize algorithms like stochastic block partitioning (SBP), which has largely limited its applicability in prior work to smaller datasets. In this work, we take a significant step towards making SBP practical on web-scale graphs by distributing its computation on multiple nodes of a computational cluster.

We first empirically show that the state-of-the-art distributed SBP algorithm, the divide-and-conquer SBP (DC-SBP) algorithm, has two conditions under which it suffers from poor convergence. The first occurs when the number of compute nodes is high, and the second occurs when the graph is sufficiently sparse. In both cases, the quality of community detection results is negatively affected, often to the point where the algorithm fails to converge entirely. This effect on convergence is largely a result of the combination of the round-robin distribution strategy and lack of inter-node communication within DC-SBP, which lead to subgraphs being independently processed with many island vertices.

We then introduce our exact distributed SBP (EDiSt) algorithm, which tackles both conditions by (a) allowing data to be duplicated across MPI tasks, and (b) allowing communication between the subgraphs being processed. We empirically show that EDiSt maintains result quality both at large numbers of MPI tasks and on sparse graphs.

Because the recombination phase of DC-SBP runs on a single node, and because EDiSt can scale to a larger number of MPI tasks without sacrificing accuracy, EDiSt is faster than DC-SBP when run on computational clusters. In our results, using 64 compute nodes and 256 MPI tasks, we achieve speedups as high as $26.9\times$ over the best-performing DC-SBP run on the same real-world graph, and as high as $23.8\times$ on the same synthetic graph. Additionally, EDiSt is up to $44.0\times$ faster than shared memory parallel SBP on a single node.

The two approaches are not antithetical. Unlike DC-SBP, EDiSt lacks a proper data distribution method. Implementing a distributed data structure for EDiSt is untrivial due to the need for both column-wise and row-wise traversal of the underlying blockmodel matrix, as well as the random memory access pattern that is a result of the randomness inherent to SBP.

In future work, we aim to improve the accuracy of DC-SBP via an improved data distribution strategy such as METIS [31] or a localized approach that approximates Voronoi decomposition on a graph. Then, each partition/subgraph can be processed at scale using EDiSt. Such a hybrid method could benefit from both the data distribution of DC-SBP and the scalability of EDiSt. We would also like to scale EDiSt to larger clusters. With a large number of nodes, the all-to-all communication patterns in EDIST are likely to present a significant bottleneck. To mitigate this, we plan to explore alternative communication approaches, including MPI one-sided communication primitives and prioritizing communication based on the Fisher information content of the edges in the graph [32].

## REFERENCES

[1] S. Fortunato, "Community detection in graphs," *Physics Reports*, vol. 486, no. 3-5, pp. 75–174, 2 2010. [Online]. Available: doi.org/10.1016/j.physrep.2009.11.002

[2] V. Oles, S. Dash, and R. Anandakrishnan, "BiGPICC: a graph-based approach to identifying carcinogenic gene combinations from mutation data," *bioRxiv*, p. 2023.02.06.527327, 2 2023. [Online]. Available: doi.org/10.1101/2023.02.06.527327

[3] B. Krishnamurthy, J. Wang, B. Krishnamurthy, and J. Wang, "On network-aware clustering of Web clients," in *ACM SIGCOMM Computer Communication Review*, vol. 30, no. 4. Stockholm, Sweden: ACM, 2000, pp. 97–110. [Online]. Available: doi.org/10.1145/347057.347412

[4] G. Rizos, S. Papadopoulos, and Y. Kompatsiaris, "Multilabel user classification using the community structure of online networks," *PLOS ONE*, vol. 12, no. 3, p. e0173347, 2017. [Online]. Available: doi.org/10.1371/journal.pone.0173347

[5] G. Li, D. Zhang, and Y. Li, "Packet Classification Using Community Detection," in *2017 IEEE International Symposium on Parallel and Distributed Processing with Applications and 2017 IEEE International Conference on Ubiquitous Computing and Communications (ISPA/IUCC)*. Guangzhou, China: IEEE, 2017, pp. 94–100. [Online]. Available: doi.org/10.1109/ISPA/IUCC.2017.00023

[6] T. P. Peixoto, "Parsimonious Module Inference in Large Networks," *Physical Review Letters*, vol. 110, no. 14, p. 148701, 4 2013. [Online]. Available: doi.org/10.1103/PhysRevLett.110.148701

[7] B. Karrer and M. E. J. Newman, "Stochastic blockmodels and community structure in networks," *Physical Review E*, vol. 83, no. 1, p. 016107, 1 2011. [Online]. Available: doi.org/10.1103/PhysRevE.83.016107

[8] T. P. Peixoto, "Efficient Monte Carlo and greedy heuristic for the inference of stochastic block models," *Physical Review E*, vol. 89, no. 1, p. 012804, 1 2014. [Online]. Available: doi.org/10.1103/PhysRevE.89.012804

[9] ——, *Descriptive vs. inferential community detection in networks: pitfalls, myths, and half-truths*. Cambridge: Cambridge University Press, 11 2023. [Online]. Available: doi.org/10.1017/9781009118897

[10] R. Guimerà, M. Sales-Pardo, and L. A. Amaral, "Modularity from fluctuations in random graphs and complex networks," *Physical Review E - Statistical Physics, Plasmas, Fluids, and Related Interdisciplinary Topics*, vol. 70, no. 2, p. 4, 8 2004. [Online]. Available: doi.org/10.1103/PhysRevE.70.025101

[11] E. Kao, V. Gadepally, M. Hurley, M. Jones, J. Kepner, S. Mohindra, P. Monticciolo, A. Reuther, S. Samsi, W. Song, D. Staheli, and S. Smith, "Streaming graph challenge: Stochastic block partition," in *2017 IEEE High Performance Extreme Computing Conference (HPEC)*. Waltham, MA: IEEE, 9 2017, pp. 1–12. [Online]. Available: doi.org/10.1109/HPEC.2017.8091040

[12] F. Wanye, V. Gleyzer, and W.-c. Feng, "Fast Stochastic Block Partitioning via Sampling," in *2019 IEEE High Performance Extreme Computing Conference (HPEC)*. Waltham, MA, USA: IEEE, 9 2019, pp. 1–7. [Online]. Available: doi.org/10.1109/HPEC.2019.8916542

[13] F. Wanye, V. Gleyzer, E. Kao, and W.-c. Feng, "On the Parallelization of MCMC for Community Detection," in *Proceedings of the 51st International Conference on Parallel Processing*. New York, NY, USA: ACM, 2022, pp. 1–13. [Online]. Available: doi.org/10.1145/3545008.3545058

[14] A. J. Uppal, J. Choi, T. B. Rolinger, and H. Howie Huang, "Faster Stochastic Block Partition Using Aggressive Initial Merging, Compressed Representation, and Parallelism Control," *2021 IEEE High Performance Extreme Computing Conference, HPEC 2021*, 2021. [Online]. Available: doi.org/10.1109/HPEC49654.2021.9622836

[15] A. J. Uppal, G. Swope, and H. H. Huang, "Scalable stochastic block partition," in *2017 IEEE High Performance Extreme Computing Conference (HPEC)*. IEEE, 9 2017, pp. 1–5. [Online]. Available: doi.org/10.1109/HPEC.2017.8091050

[16] T. P. Peixoto, "Entropy of stochastic blockmodel ensembles," *Physical Review E*, vol. 85, no. 5, p. 056122, 5 2012. [Online]. Available: doi.org/10.1103/PhysRevE.85.056122

[17] W. K. Hastings, "Monte Carlo sampling methods using Markov chains and their applications," *Biometrika*, vol. 57, no. 1, pp. 97–109, 4 1970. [Online]. Available: doi.org/10.1093/biomet/57.1.97

[18] A. Terenin, D. Simpson, and D. Draper, "Asynchronous Gibbs Sampling," in *International Conference on Artificial Intelligence and Statistics*. Palermo: PMLR, 6 2020, pp. 144–154. [Online]. Available: doi.org/10.48550/arXiv.1509.08999

[19] S. van der Walt, S. C. Colbert, and G. Varoquaux, "The NumPy Array: A Structure for Efficient Numerical Computation," *Computing in Science & Engineering*, vol. 13, no. 2, pp. 22–30, 3 2011. [Online]. Available: doi.org/10.1109/MCSE.2011.37

[20] L. Dalcín, R. Paz, M. Storti, and J. D'Elía, "MPI for Python: Performance improvements and MPI-2 extensions," *Journal of Parallel and Distributed Computing*, vol. 68, no. 5, pp. 655–662, 5 2008.

[21] X. Yu, H. Wang, W. c. Feng, H. Gong, and G. Cao, "GPU-Based Iterative Medical CT Image Reconstructions," *Journal of Signal Processing Systems*, vol. 91, no. 3-4, pp. 321–338, 3 2019. [Online]. Available: doi.org/10.1007/S11265-018-1352-0

[22] L. DeRose, B. Homer, and D. Johnson, "Detecting application load imbalance on high end massively parallel systems," *Lecture Notes in Computer Science (including subseries Lecture Notes in Artificial Intelligence and Lecture Notes in Bioinformatics)*, vol. 4641 LNCS, pp. 150–159, 2007. [Online]. Available: doi.org/10.1007/978-3-540-74466-5_17

[23] T. P. Peixoto, "The graph-tool python library," *figshare*, 2014. [Online]. Available: doi.org/10.6084/m9.figshare.1164194

[24] J. Leskovec and A. Krevl, "SNAP Datasets: Stanford Large Network Dataset Collection," 2014. [Online]. Available: snap.stanford.edu/data/

[25] P. Boldi, B. Codenotti, M. Santini, and S. Vigna, "UbiCrawler: a scalable fully distributed Web crawler," *Software: Practice and Experience*, vol. 34, no. 8, pp. 711–726, 7 2004. [Online]. Available: doi.org/10.1002/spe.587

[26] P. Boldi and S. Vigna, "The webgraph framework I: compression techniques," in *13th international conference on World Wide Web*. Association for Computing Machinery (ACM), 5 2004, pp. 595–602. [Online]. Available: doi.org/10.1145/988672.988752

[27] P. Boldi, M. Rosa, M. Santini, and S. Vigna, "Layered label propagation: A multiresolution coordinate-free ordering for compressing social networks," *Proceedings of the 20th International Conference on World Wide Web, WWW 2011*, pp. 587–596, 2011. [Online]. Available: doi.org/10.1145/1963405.1963488

[28] "SuiteSparse Matrix Collection." [Online]. Available: https://sparse.tamu.edu/

[29] N. Stanley, R. Kwitt, M. Niethammer, and P. J. Mucha, "Compressing Networks with Super Nodes," *Scientific Reports*, vol. 8, no. 1, p. 10892, 12 2018. [Online]. Available: doi.org/10.1038/s41598-018-29174-3

[30] A. S. Maiya and T. Y. Berger-Wolf, "Sampling community structure," in *Proceedings of the 19th international conference on World wide web - WWW '10*. New York, New York, USA: ACM Press, 2010, p. 701. [Online]. Available: doi.org/10.1145/1772690.1772762

[31] G. Karypis and V. Kumar, "A Fast and High Quality Multilevel Scheme for Partitioning Irregular Graphs," *SIAM Journal on Scientific Computing*, vol. 20, no. 1, pp. 359–392, 1 1998. [Online]. Available: doi.org/10.1137/S1064827595287997

[32] E. K. Kao, S. T. Smith, and E. M. Airoldi, "Hybrid Mixed-Membership Blockmodel for Inference on Realistic Network Interactions," *IEEE Transactions on Network Science and Engineering*, vol. 6, no. 3, pp. 336–350, 7 2019. [Online]. Available: doi.org/10.1109/TNSE.2018.2823324